Journal of AgriSearch, 13 (2) : 117-123
An Open Access International Peer Reviewed Quaterly

ISSN : 2348-8808 (Print), 2348-8867 (Online)
https://doi.org/10.21921/jas.v13i02.15282

Non-destructive Modeling of Mango Geometrical Attributes Assessed Using Image Processing Technique for Mass and Volume Measurement

Krishna Kumar Patel[1*] and Abhijit Kar[2]

ABSTRACT

The mechanization of post-harvest operations and the management of mangoes are crucial for minimizing post-harvest losses. Economic factors, the quality of the fruit, and the reputation of mango growers and exporting countries are significantly impacted by traditional sorting and grading techniques. Therefore, obtaining quick and accurate geometrical data is essential for designing equipment for sorting, grading, loading, unloading, and packaging mangoes after harvest. This study focuses on capturing images using a near-infrared (NIR) camera, processing those images, and analyzing external dimensions (length, breadth, and thickness) using LabVIEW software. The geometrical attributes obtained were then utilized for non-destructive modeling of mango mass and volume. The correlation strength, indicated by the R value of the calibration regression equation, ranged from 0.634 to 0.932 for mass, and from 0.624 to 0.805 for fruit volume. The findings indicated that the best mass models were based on the length, arithmetic mean diameter, and all three external dimensions (length, breadth, and thickness). Conversely, the volume models that provided the best fit were based on the length and breadth of the fruits.

Keywords: Assessment, Human vision, Mango, Non-destructive, Physical quality, Rapid

ARTICLE INFO

Received on	:	18/04/2026
Accepted on	:	05/06/2026
Published online	:	30/06/2026

INTRODUCTION

Fresh fruits and vegetables play a vital role in maintaining human health by providing essential vitamins, minerals, plant compounds, and fiber. Numerous studies have shown that a diet rich in fruits and vegetables can protect against serious diseases such as cancer, diabetes, and heart disease. Among these, the mango is renowned for its delicious flavor, juiciness, and various health benefits (Patel and Kar, 2023). Consuming mangoes can boost the immune system, lower cholesterol, and help prevent digestive issues. Additionally, the high levels of vitamin A (carotene) in mangoes make them excellent for improving eyesight. However, ensuring the quality and freshness of mangoes in the market is a significant concern. The traditional manual methods used for post-harvest operations are time-consuming, which delays the availability of mangoes and can result in considerable post-harvest losses. To mitigate these losses and maintain freshness, real-time sorting and grading processes are essential for improving operational efficiency (Patel and Pathare, 2024). There are several non-destructive, real-time, image processing techniques available in the public domain. Most of these techniques utilize color cameras, which tend to be more expensive and somewhat slower than near-infrared (NIR) monochrome imaging systems. NIR imaging is similar to human vision but excludes color wavelengths; thus, objects, after removing color, often resemble black-and-white images. The NIR imaging system offers excellent sensitivity and high contrast in challenging lighting conditions, all at a lower cost compared to CCD cameras. Additionally, due to its unique spectral characteristics, NIR imaging produces high-quality results (Patel et al., 2012). This system is capable of collecting over 80,000 spectra per minute, and with appropriate software and robust statistical analysis, valuable information can be extracted from the resulting data (Guzman et al., 2026). In the food industry, infrared imaging has various applications, such as assessing the properties of foodstuffs (including firmness, soluble solids, and acidity) and identifying foreign objects in food products. Many physiological properties of food are strongly correlated with infrared signals. Analysing thermograms is effective for evaluating quality and shelf life in fruits and vegetables. Therefore, NIR imaging presents a promising alternative technology for non-destructive applications (Patel and Kar, 2022). The market for NIR imaging is expected to increase from 285 million USD in 2019 to 485 million USD by 2030, underscoring its importance in

[1]Department of Processing and Food Engineering, B.S.Dr.B.R.A. College of Agricultural Engineering and Technology (Etawah-206 001), C.S.AU.A. & T., Kanpur, Uttar Pradesh, (India)
[2]Director, National Institute of Secondary Agriculture, Namkum, Ranchi (India)
[*]Corresponding Author E-mail: k_krishna_374@yahoo.co.in

determining the quality of agricultural and food products (Patel and Pathare, 2024). NIR imaging-based CVS (computer vision system) could also help manage food logistics (Chen et al., 2009).

A near-infrared imaging system was developed by Lin et al. (2006) to determine the moisture content of rice. Their findings indicated that the performance of the near-infrared (NIR) imaging system was almost identical to that of near-infrared spectrometry (NIRS). McClure (1987) also used the NIR system to measure moisture content in rice. Consequently, NIR imaging systems can be employed to predict various properties and detect defects. However, a significant drawback of the NIR imaging system is its requirement for frequent calibration, as it is highly sensitive to moisture content variations in samples (McClure, 1987). In addition, Jirsa et al. (2007) explored the bakery characteristics of wheat dough and its final products using NIR imaging techniques. They reported that these techniques could also predict protein content and zeleny sedimentation.

As an indirect method, NIR imaging can, thus, be utilized in arable crops to detect and locate insect infestations. But it is ineffective at identifying low levels of infestation in bulk samples containing both live and dead insects (Dowell et al., 1999). Ridgway and Chambers (1998) employed an NIR videocon camera to capture images of infested wheat samples, detecting insects through a comparative method. Similarly, Davies et al. (2003) assessed the potential of NIR imaging for identifying and locating insects in cereal grains, proposing a line segment detection method that requires minimal computation. Schmilovitch et al. (2000) also applied NIR imaging within an appropriate spectral range to evaluate specific physiological properties of mangoes var, Tommy Atkins. Further, light penetration into the upper layer and the ability to visualize the targeted area of objects are two fundamental advantages of the NIR spectrum of electromagnetic waves. Numerous studies have demonstrated the importance of the non-destructive system based on both visible and non-visible imaging in detecting fruit quality defects. NIR imaging can help visualize biological tissues and hidden defects just below the peel by reducing the artifacts caused by light illumination (Patel and Pathare, 2024).

Overall, non-destructive techniques based on the NIR system can effectively measure food properties in a very short time frame without the need for sample preparation. This approach can be successfully integrated throughout the food industry, with the primary advantage being the ability to estimate multiple quality parameters simultaneously (Lammertyn et al., 1998). Because of its versatility, NIR imaging can be used to solve problems in a wide range of fields, including computer vision, automation, life sciences, medicine, license plate recognition, and security. When visible cameras malfunction, for instance, it helps with packaging inspection and defect detection.

Considering the above facts, the main objectives of this study were to use computer vision (CV) based on the near infrared (NIR) image processing technique, which is very close to human vision, to extract the geometrical information of mangoes and to model these geometric attributes for the non-destructive measurement of the mass and volume of mangoes.

MATERIALS AND METHODS

Mangoes from Chausa and Dashehari were chosen for this study because of their peel colour and production traits, which make them ideal for image processing. To reduce transportation delays, sixty ripe fruits were purchased from neighbouring orchards. Using vernier callipers (least count: 0.01 mm; model no. CD-6" CSX Mitutoyo, Japan), we measured each fruit's length (L), width (W), and thickness (T) in the lab. Additionally, we used a near-infrared (NIR) camera to take six pictures of each fruit: four from a 90-degree rotation, one from the top, and one from the bottom. Below are more specifics about the NIR computer vision (NIR CV) system.

Description of NIR computer vision system

This study made use of an imaging (computer vision) system fabricated in the Indian Agricultural Research Institute's Division of Post-Harvest Technology in New Delhi, India. In this study, a visible lighting regime consisting of nine fluorescent bulbs (50 watts, 220 volts) arranged in a cylindrical configuration was combined with the NIR camera. However, electronic ballasts and an uninterrupted power supply (UPS) system were used to guarantee a steady supply of electricity. Mango fruits that have been manually placed are captured by the camera, which was placed at the top of the illumination chamber. An industrial computer with a frame grabber receives the video signal from the camera and uses it to take pictures. Every image is kept in TIFF (Tagged Image File Format) in the hardware memory of the computer. The location of the detected objects' centers is ascertained by the computer, and this data is used for additional processing. Thus, the described system integrates an illumination chamber, an NIR camera, visible lighting, a frame grabber, image processing and analysis software, and computer hardware.

Computer features (H/W and S/W)

An industrial PC with an LED screen and a 320 x 256 pixel NIR camera (Model: NIR-300GE; Vosskohler GmbH, Germany) were used in this study. The camera was placed in the illumination chamber approximately 200 mm above the fruit and connected to the PC via a Gigabit Ethernet port via a Cat5e cable. The computer's memory was used to store pictures of the mango fruit on the sample platform. The camera was positioned 59 cm above the floor of the chamber. For image processing and analysis, we used the IMAQ Vision library

from LabVIEW (National Instruments, Austin, TX).

Processing of images

Algorithms were developed for processing NIR images of Chausa and Dashehari fruits. The images were initially sub-sampled to 99×81 pixels for Chausa and 81×58 pixels for Dashehari to reduce computational time. Brightness was enhanced using values of 66 for brightness, 45.50° for contrast, and 0.41 for gamma to clarify the images.

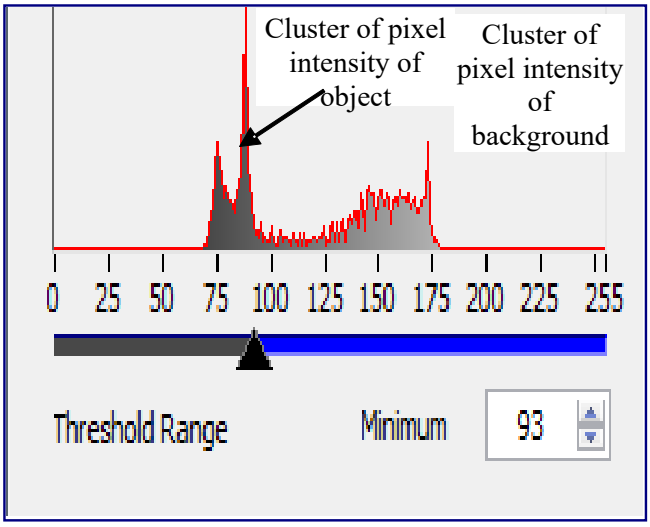

(i) Chausa Fruits

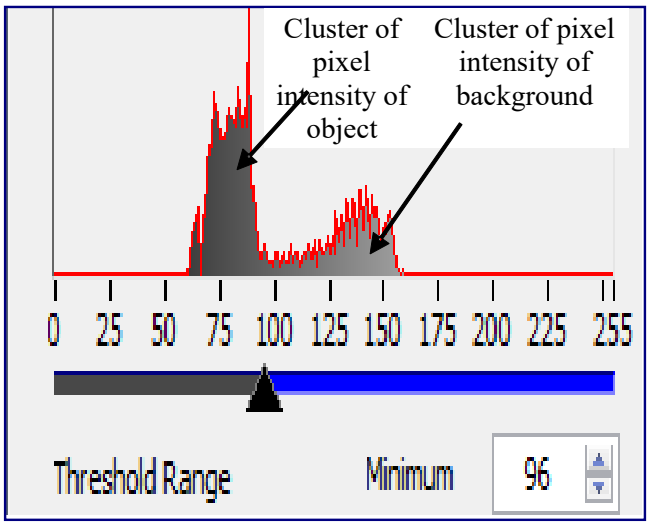

(ii) Dashehari Fruits

Fig. 1: Histogram displays threshold value of manual threshold set up looking for bright objects (i.e. fruit)

highest contrast between the fruits and the background. However, obtaining a proper bimodal histogram proved to be challenging. To separate the bright fruit (foreground) from the dark background, a manual threshold operation was performed, setting maximum thresholds at 96 for Chausa and 93 for Dashehari. Figure 2 illustrates the image processing and analysis operations employed in these algorithms. A lookup table operation was used to equalize the grayscale values to enhance the image details in areas containing significant information. Although the equalized image was sometimes useful for the direct detection of defects, challenges arose due to light intensity gradients, poor contrast, irregular interfaces, and touching blemishes, all of which needed to be addressed for the algorithm's accuracy. The equalized image was subsequently filtered using a smoothing median filter with a 15×15 size, along with a Sobel filter (with a 3×3 kernel size) to determine the horizontal and vertical gradients, which were then used for boundary tracing of the objects.

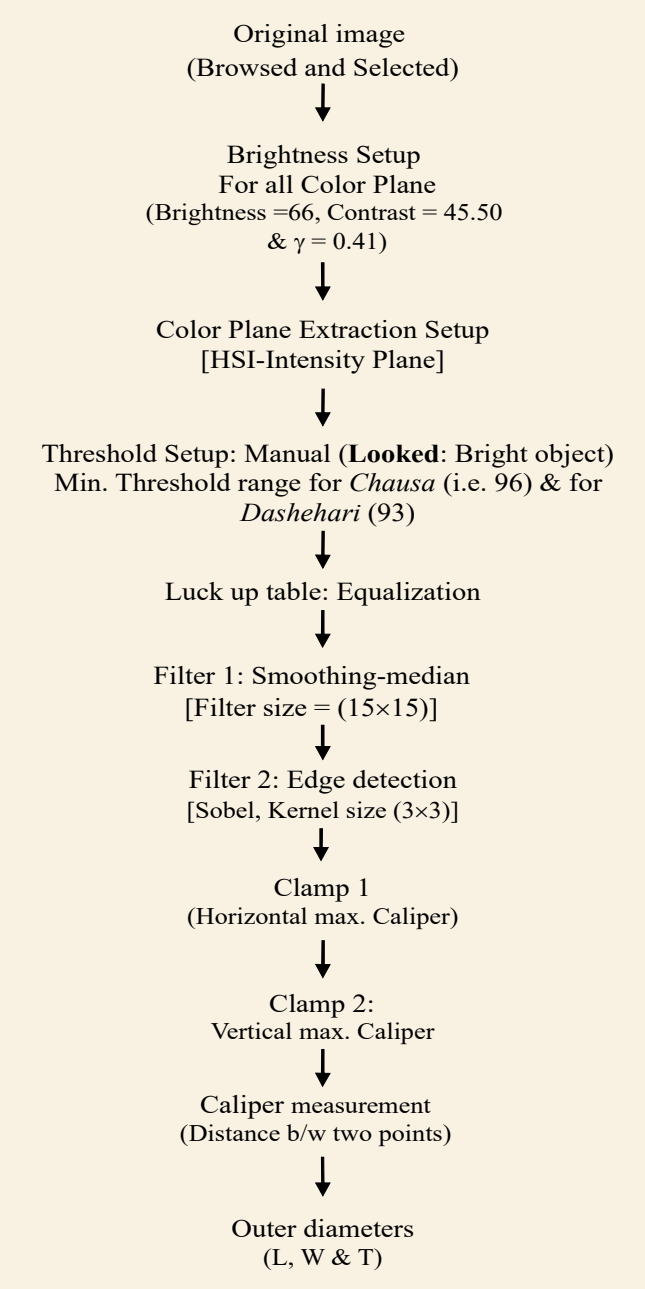

Fig. 1: Flow diagram of the algorithm for measuring dimensions in Chausa (A) and Dashehari (B) Fruit using NIR CVS

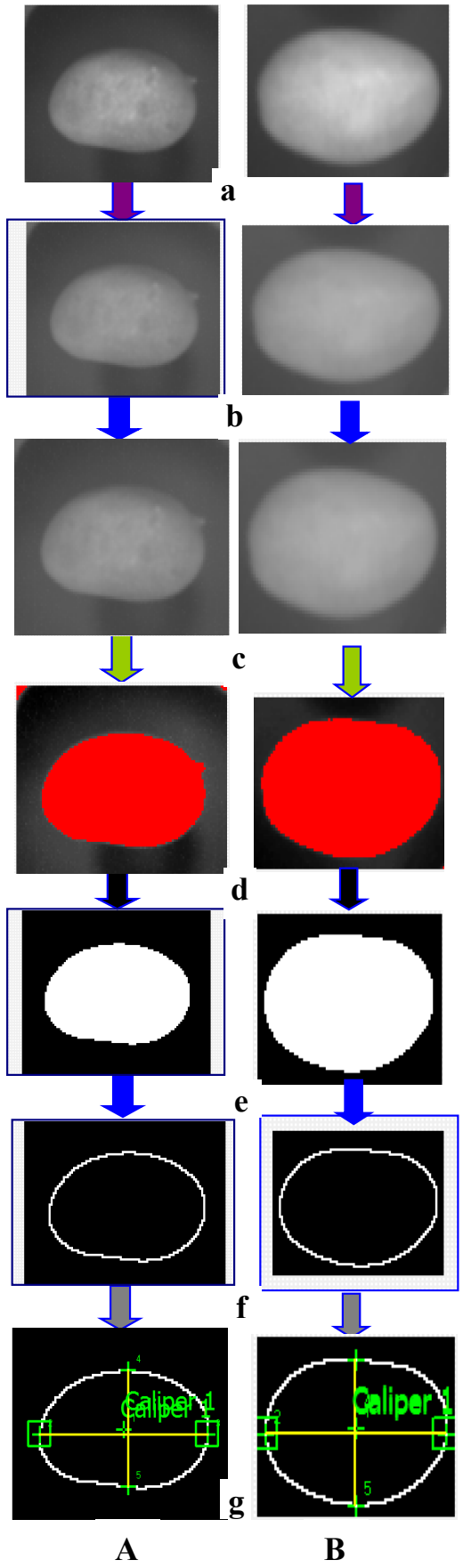

Finally, a rake-based clamp and caliper function, which operates only with an 8-bit machine, was employed to find edges along a rectangular region of interest (ROI) by drawing on the image and measuring the distance between the first and last edges found. Additionally, various morphological measurements were extracted from the fruit images after applying noise reduction, utilizing a particle analysis technique in IMAQ Vision software. Based on the aforementioned image processing steps, a flow diagram was developed to illustrate the algorithms for the physical characterization of Chausa and Dashehari fruits. The steps in this process include: (a) the original NIR image, (b) the image after brightness enhancement, (c) the image after HIS intensity plane extraction, (d) the image after threshold application, (e) the filtered image, (f) the outline of the image, and (g) the image displaying length and breadth measurements.

RESULTS AND DISCUSSION

External Diameters of Mango Fruit

This study evaluated a near-infrared-based computer vision system for assessing the physical quality parameters of Chausa and Dashehari mango cultivars. Images of the fruits were captured and cropped to dimensions of 99×81 pixels for Chausa and 81×58 pixels for Dashehari to reduce costs and computational time.

Table 1: The mean values, standard deviation (S.D.) and range (min, max) of some geometric attributes of mango fruits (var. Chausa) analyzed by IP techniques using NIR CVS

Parameters	NIR camera based CVS			
	Mean	Minimum	Maximum	Standard deviation
***Chausa* cultivar**				
Length (mm)	107.94	80.40	95.78	6.43
Breadth (mm)	52.54	47.73	56.43	3.68
Thickness (mm)	57.69	33.27	48.70	3.74
AMD, mm	67.10828	57.28438	73.91146	4.1403
GMD, mm	64.21159	52.77669	71.45375	4.060033
AR	59.7447	52.04855	69.4891	3.724529
Sphericity	67.2448	59.39559	72.99568	3.006982
Area (mm^2)	5287.593	4366	6590	646.2825

Morphological features such as length, width, and thickness were analyzed after processing the fruit images through segmentation. The algorithms used in LabVIEW for analyzing the fruits are illustrated in Figure 2. Key measurements of the outer diameters are critical for classifying and pricing the fruits. The lengths for the Chausa mango ranged from 80.40 mm to 107.94 mm (Table 1), while the Dashehari ranged from 75.27 mm to 114.78 mm, with standard deviations of 6.43 mm and 9.85 mm (Table 2), respectively. Dashehari exhibited both the shortest and longest fruits in the study. Statistical analysis indicated that Dashehari fruits are slightly bulkier than Chausa. There was significant variation in the length of Dashehari fruits, while the variation in their width was the lowest among the measured diameters.

Table 2: The mean values, standard deviation (S.D.) and range (min, max) of some geometric attributes of mango fruits (var. dashehari) analyzed by IP techniques using NIR CVS

Parameters	NIR camera based CVS			
	Mean	Minimum	Maximum	Standard deviation
Length (mm)	97.54	75.27	114.78	9.85
Breadth (mm)	55.89	51.29	60.96	2.45
Thickness (mm)	50.73	45.69	55.70	2.96
AMD, mm	67.95386	58.13204	74.57181	3.966178
GMD, mm	64.9472	56.94668	69.77332	3.149243
AR	57.96613	49.43286	72.1409	6.080482
Sphericity	67.17841	58.91899	76.18283	5.080888
Area (mm2)	5505.63	4511.00	6536	620.06

Furthermore, in order to estimate mass/ mass and volume of fruits using image processing technique, CVS based on NIR image acquisition system can also be used. On the basis of geometrical attributes extracted from NIR mango image profile, fourteen models were suggested for estimation of fruits mass and volume of *Chausa* and *dashehari* cultivars (Table 3, 4). Fruits from both cultivars were considered in combination for developing of these models.

Mass modeling

The r value of calibration/validation regression equation for mass was noticed between 0.634-0.932 and 0.616-0.926, respectively. The lowest coefficient of correlation was obtained for the thickness or minor diameter (model no. 3) of mango fruits extracted from the profile image acquired by NIR camera. This suggests that only 63% variation in fruits mass can be explained by the model no. 3. In contrast, length (major diameter) of fruits has good correlation (0.81) and width (intermediate diameter) of fruits has reasonable correlation with the mass. The maximum correlation coefficient was found for the model no. 8, 10, 11, 12, 13 and 14 while minimum was found for the regression equation based on thickness of the fruits.

Further, model number 8 can be chosen as the best model due to its use of a single variable (Da) in the regression equation, lower SEC/SEP value (10.68/10.93), lowest difference between SEC and SEP (0.25), and higher R value (0.907). Based on the highest R value (0.932), lower SEC/SEP value (10.66/11.04), and lower difference between SEC and SEP (0.28), model number 13 can also be chosen as one of the best models. However, because this model (number 13) is based on fruit length and geometric mean diameters, it is more complicated than model number 8. To put it another way, the sizing mechanism is complicated, laborious, expensive, and time-consuming because model no. 13 is based on all three diameters and measurement of each is required. The mass of the fruits of the Chausa and Dashehari cultivars can also be predicted using model nos. 10 and 11. All models were found to be a reasonable fit of the data, with the exception of model number three.

Table 3: Various MLR models based on IP dimensional characteristics (length, breadth and thickness) for determining mass of mango fruits of Chausa and dashehari cultivars

S. No.	Models	Relation	SEC/SEP	Bias	Correlation			
			Calibration	Validation	Calibration	Validation	Calibration	Validation
1	$M=K_1L+K_2$	$M=2.48\,L-56.79$	14.79	15.17	-0.000	0.016	0.812	0.802
2	$M=K_1W+K_2$	$M=5.12\,W-128.70$	17.39	17.34	0.000	0.016	0.718	0.708
3	$M=K_1T+K_2$	$M=3.943\,T-12.93$	18.86	19.30	0.000	-0.022	0.637	0.616
4	$M=K_1LW+K_2$	$M=3.16x10^{-2}\,LW+0.42$	12.24	12.53	0.000	0.009	0.876	0.869
5	$M=K_1LT+K_2$	$M=3.16x10^{-2}\,LT+9.24$	12.43	12.72	-0.000	-0.009	0.872	0.865
6	$M=K_1LWT+K_2$	$M=4.92x10^{-4}\,LWT+48.38$	11.99	12.26	0.000	0. 006	0.881	0.875
7	$M=K_1D_g+K_2$	$M=6.0\,D_g-202.45$	12.07	12.37	-0.000	-0.027	0.879	0.873

S. No.	Models	Relation	SEC/SEP	Bias	Correlation			
			Calibration	Validation	Calibration	Validation	Calibration	Validation
8	$M=K_1D_a+K_2$	$M=5.6\,D_a-199.28$	10. 68	10. 93	-0.000	-0.008	0.907	0.903
9	$M=K_1L+K_2T+K_3$	$M=2.20\,L+2.43T-150.41$	11.52	11.92	0.000	-0.016	0.891	0.883
10	$M=K_1L+K_2W+K_3T+K_4$	$M=1.97\,L+1.72W+1.78T-193.92$	10.64	11.18	-0.000	0.013	0.908	0.898
11	$M=K_1L+K_2WT+K_3$	$M=1.98\,L+3.33\times10^{-2}\,WT-102.55$	10.59	10.97	0.000	-0.022	0.909	0.902
12	$M=K_1L+K_2LWT+K_3$	$M=1.02\,L+3.49\times10^{-4}\,LWT-11.39$	10.65	11.04	0.000	-0.017	0.907	0.900
13	$M=K_1L+K_2D_g+K_3$	$M=1.04\,L+4.20\,D_g-189.62$	10.66	11.04	0.000	-0.039	0.932	0.926
14	$M=K_1L+K_2D_a+K_3$	$M=0.22\,L+5.26\,D_a-194.01$	10.64	11.02	0.000	-0.029	0.908	0.901

Table 4: Various MLR models based on IP dimensional characteristics (length, breadth and thickness) for determining volume of mango fruits of Chausa and dashehari cultivars

S. No.	Models	Relation	SEC/SEP	Bias	Correlation			
			Calibration	Validation	Calibration	Validation	Calibration	Validation
1	$V=K_1\,L+K_2$	$V=2.40\,L-52.09$	18.73	19.26	0.000	0.014	0.708	0.688
2	$V=K_1\,W+K_2$	$V=5.33\,W-123.21$	20.27	20.73	0.000	0.012	0.647	0.626
3	$V=K_1\,T+K_2$	$V=3.654\,T+6.73$	20.07	20.50	0.000	0.012	0.624	0.604
4	$V=K_1\,LW+K_2$	$V=3.72\times10^{-2}\,LW+0.138$	15.67	16.12	0.000	0.013	0.805	0.792
5	$V=K_1\,LT+K_2$	$V=3.14\times10^{-2}\,LT+27.99$	18.07	18.59	-0.000	0.095	0.728	0.709
6	$V=K_1\,LWT+K_2$	$V=4.34\times10^{-4}\,LWT+59.82$	17.45	17.94	0.000	0. 081	0.749	0.733
7	$V=K_1\,D_g+K_2$	$V=5.35\,D_g-167.70$	17.10	17.54	-0.000	0.057	0.761	0.746
8	$V=K_1\,D_a+K_2$	$V=4.82\,D_a-147.68$	17.56	18.10	0.000	0.075	0.745	0.727
9	$V=K_1\,L+K_2\,T+K_3$	$V=1.47\,L+3.18\,T-121.46$	17.72	18.51	-0.000	-0.020	0.740	0.712
10	$V=K_1\,L+K_2\,W+K_3\,T+K_4$	$V=1.22\,L+1.90\,W+2.46\,T-169.25$	17.04	18.00	0.000	0.032	0.763	0.731
11	$V=K_1\,L+K_2\,WT+K_3$	$V=1.21\,L+4.21\times10^{-2}\,WT-56.64$	17.09	17.88	-0.000	-0.023	0.761	0.735
12	$V=K_1\,L+K_2\,LWT+K_3$	$V=5.58\times10^{-2}\,L+4.27\times10^{-4}\,LWT+56.56$	17.45	17.28	0.000	0.029	0.749	0.721
13	$V=K_1\,L+K2\,D_g+K_3$	$V=1.14\times10^{-2}\,L+5.33\,D_g-167.53$	17.10	17.88	-0.000	0.003	0.761	0.735
14	$V=K_1\,L+K_2\,D_a+K_3$	$V=1.044\,L+6.69\,D_a-173.38$	17.06	17.85	0.000	0.014	0.762	0.736

Modeling of mango fruit's volume

The models recommended for volume estimation are displayed in Table 2. Based on strong correlation, model no. 4 can be chosen as the best model because it had the highest R value (0.805) and the lowest SEC/SEP value (15.67/16.12). The two fruit diameters must be assessed in order to estimate fruit volume because this model is based on the multiplication of two variables, namely IP length (L) and width (W). On the other hand, models no. 1, 2, and 3, which were based on a single fruit diameter (L, W, and T), were straightforward, economical, and time-efficient; however, their degree of correlation was somewhat lower. Furthermore, models 7, 10, 11, 13, and 14 have R values greater than 0.75, suggesting a reasonable and positive correlation strength.

Additionally, there was no discernible bias in the calibration or validation regression equations for volume estimation, with correlation coefficients ranging from 0.624/0.604 to 0.805 to 0.792. Similarly, Table 2 makes it clear that models based on multiple fruit diameters or variables have a stronger degree of relationship than those based on just one.

Further, during the mass and volume modeling, the AMD, GMD, aspect ratio, sphericity, and total surface area of mango fruits (Chausa and Dashehari cultivars) assessed by IP techniques using a near-infrared computer vision system were tested. However, a weak correlation between these parameters and the mass and volume was discovered. Since the model relies on these parameters, it is not discussed in this thesis.

CONCLUSION

This study explores a non-invasive near-infrared image-processing method for rapid mass and volume measurement, which supports the mechanization of sorting and grading, reducing post-harvest losses and improving growers' financial viability. Traditional sorting methods can adversely affect fruit quality and the reputation of exporting nations. Using a near-infrared (NIR) camera and LabVIEW software, mango dimensions were analysed to develop non-destructive models for mass and volume. A total of 28 models were developed, with the arithmetic mean diameter model performing best for mass measurement (r = 0.907) and the length- and width-based model for volume measurement (r = 0.805). Thirteen models for mass and twelve for volume were reasonably well fitted to the data, with correlation coefficients ranging from 0.634 to 0.932 for mass and 0.624 to 0.805 for volume.

ACKNOWLEDGEMENT

This work was supported by the National Agricultural Innovation Project, Indian Council of Agricultural Research through its subproject entitled "Development of non destructive system for evaluation of microbial and physico chemical quality parameters of mango" (C1030). In addition, I thanks to late (Dr.) Mohammad Ali Khan, the Professor in the Department of Post Harvest Engineering and Technology AMU, Aligarh who was the mentor and supervisor of my research work.

REFERENCES

Chen M H, Zhang G P and Xia H. 2009. Application of near-infrared image processing in agricultural engineering. In PIAGENG 2009: image processing and photonics for Agricultural Engineering 7489: 19–25.

Davies E R, Bateman M, Mason D R and Chambers J. 2003. Design of efficient line segment detectors for cereal grain inspection. Pattern Recognition Letters 24(1-3): 413-428.

Dowell F E, Throne J E, Wang D and Baker J E. 1999. Identifying stored grain insects using near-infrared spectroscopy. J. of Economic Entomology 92: 165–169.

Guzman U H, Rykær M, Hendriks I A, Stewart H, Denisov E, Hagedorn B, Petzoldt J, Kreutzmann A, Mueller Y, Arrey T N, Colonius I, Ostergaard O, Koenig C, Kraegenbring J, Fort K L, Couzijn E, Hauschild J P, Hermanson D, Zabrouskov V, Hock C, Damoc E and Olsen J V. 2026. Higher-Throughput Proteome Profiling Enabled by Parallelized Pre-Accumulation and Optimized Ion Processing in the Orbitrap Astral Zoom Mass Spectrometer. Molecular & Cellular Proteomics 101504.

Jirsa O, Hruskova M and Svec I. 2007. Bread features evaluation by NIR analysis. Czech J. Food Science 25: 243–248.

Lammertyn J, Nicolaï B, Ooms K, Smedt V and Baerdemaeker J. 1998. Nondestructive measurement of acidity, soluble solids, and firmness of jonagold apples using NIR-spectroscopy. Transactions of the ASAE 41(4): 1089-1094.

Lin L H, Lu F H and Chang Y C. 2006. Development of a Near Infrared Imaging System for Determination of Rice Moisture. Cereal Chemistry 83(5): 498-504.

McClure W F. 1987. Near-infrared instrumentation. In P. Williams & K. Norris (Eds.), Near-infrared technology in the agricultural and food industries (pp. 89–105). St. Paul, MN: American Association of Cereal Chemists, Inc.

Patel K K and Kar A. 2022. Potential of NIR computer vision technique for the detection of mango's defects. Journal of AgriSearch 9(4): 314-319.

Patel K K and Kar A. 2023. Studies on variability of physico-biochemical parameters of mango fruit: physico-biochemical variability in mango fruit. Journal of AgriSearch 10(1): 29-36.

Patel K K and Pathare P B. 2024. Principle and applications of near-infrared imaging for fruit quality assessment—An overview. International Journal of Food Science and Technology 59(5): 3436-3450.

Patel K K, Kar A and Khan M A. 2012. Nondestructive food quality evaluation techniques: principle and potential. Agricultural Engineering Today 36:29–34.

Ridgway C and Chambers J. 1998. Detection of insects inside wheat kernels by NIR imaging. J. Near infrared Spect. 6: 115–129.

Schmilovitch Z, Mizrach A, Hoffman A, Egozi H and Fuchs Y. 2000. Determination of mango physiological indices by near-infrared spectrometry. Postharvest biology and technology 19: 245-252.

Citation: Patel K K and Kar A.2026. Non-destructive modeling of mango geometrical attributes assessed using image processing technique for mass and volume measurement. Journal of AgriSearch 13(2):117-123.